On the Application of Basalt-Fiber Reinforced Polymer (BFRP) Bars to Prestressed Slab Elements Typical of the Precast Concrete Industry

Bruno Dal Lago, Davide Bisi and Liberato Ferrara

Department of Civil and Environmental Engineering, Politecnico di Milano

Introduction

Basalt Fibre Reinforced Polymer (BFRP) bars

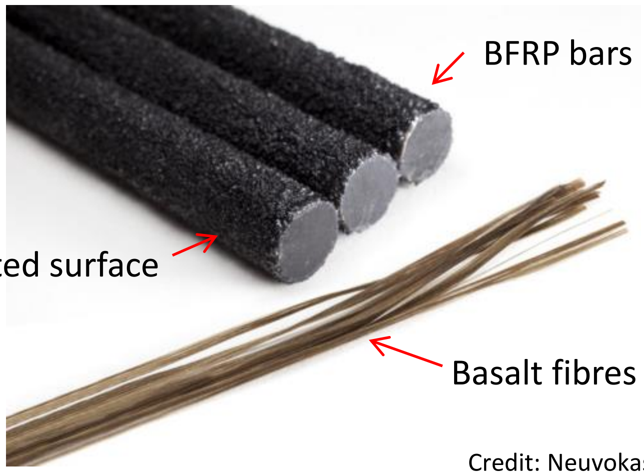

Credit: Neuvokas

Why BFRP bars in Concrete?
- Corrosion Resistant
- Low Carbon Footprint

Why BFRP bars to Pre-Stress Concrete?
- High Strength
- Low Elastic Modulus (low losses)

Property	Pre-stressing steel wire	BFRP
Yield strength (MPa)	1470-1650	N/a
Ultimate strength (MPa)	**1670-1860**	**920-1650**
Elastic modulus (GPa)	**195**	**45-59**
Yield Strain (%)	0.14-0.25	N/a
Rupture strain (%)	6-12	1.6-3.0

ISSUES:
- Unknown behaviour under sustained stress
- Problematic anchorage due to orthotropic behaviour

Credit: Crossett et al., 2015

Previous experience with BFRP in pre-tensioned precast slabs

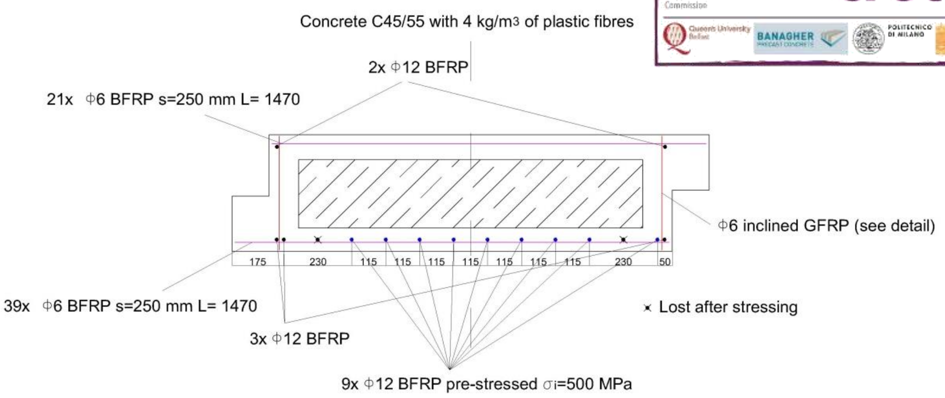

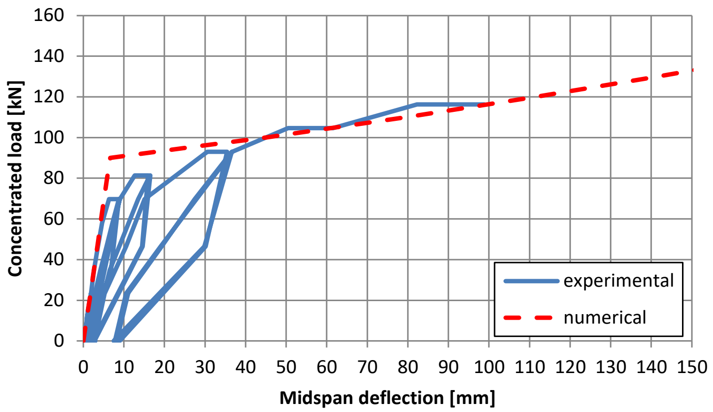

* Dal Lago B, Taylor SE, Deegan P, Ferrara L, Sonebi M, Crosset P, Pattarini A. Full-scale testing and numerical analysis of precast fibre reinforced self-compacting concrete slab pre-setressed with basalt fibre reinforced polymer bars. Composites Part B 2017.

Previous experience with BFRP in pre-tensioned precast slabs

Midspan point load = 120 kN

Almost perfect **elastic recovery** at the end of the test

Contribution of **polypropylene fibres** in distributing the cracks: **short spacing** and **small opening**

* Dal Lago B, Taylor SE, Deegan P, Ferrara L, Sonebi M, Crosset P, Pattarini A. Full-scale testing and numerical analysis of precast fibre reinforced self-compacting concrete slab pre-setressed with basalt fibre reinforced polymer bars. Composites Part B 2017.

Objectives

- Analysis of the possible use of BFRP reinforcement in the precast concrete building industry
- Design comparison between steel and BFRP prestressing reinforcement given 4 typical solutions for roofs and floors
- Characterization of the failure mechanism of the different elements
- Characterization of the service behavior of the different elements

Sections and slab arrangements

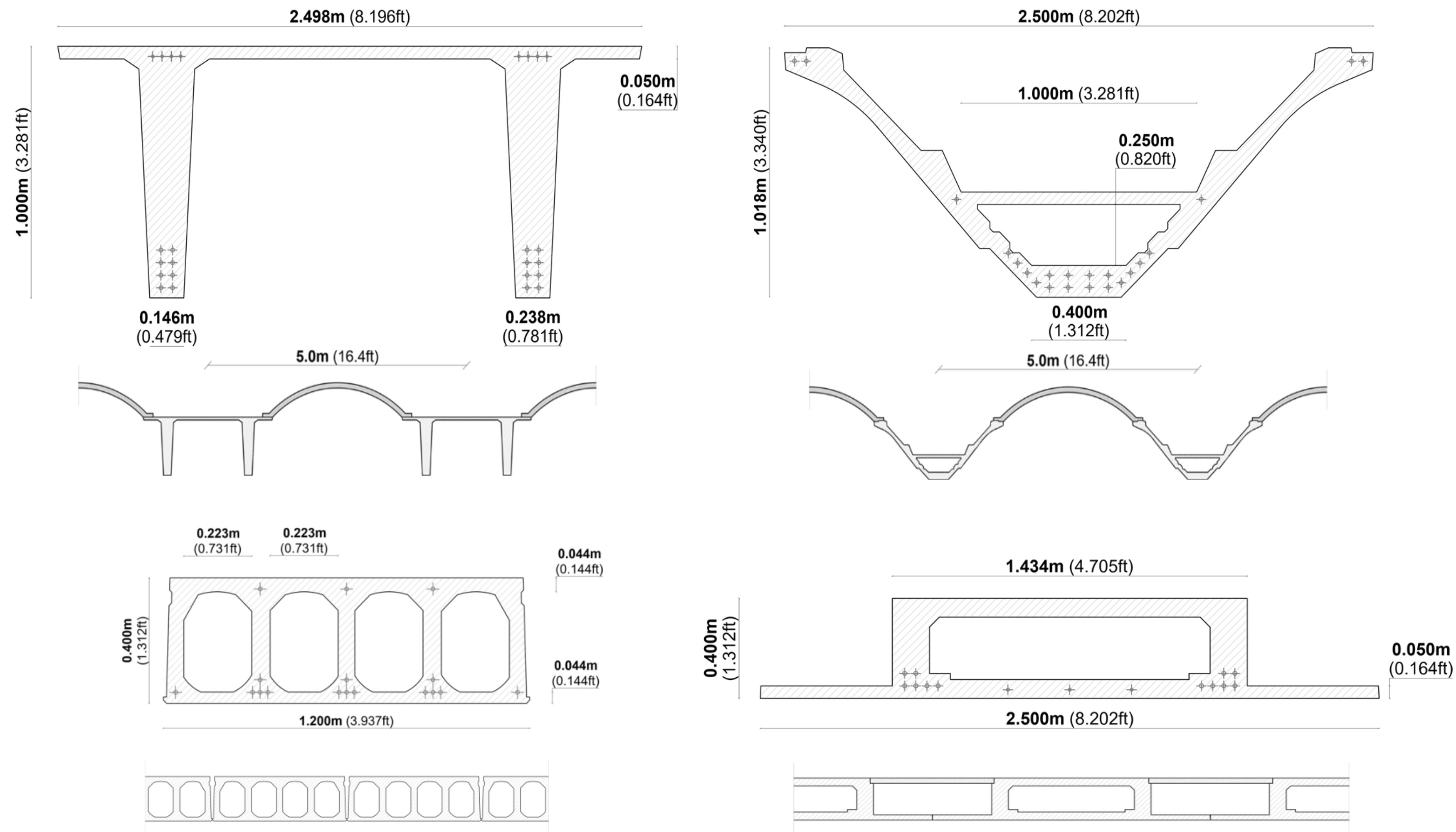

Loads and load combinations

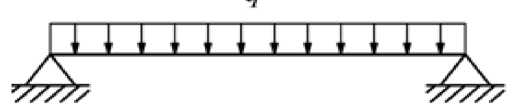

	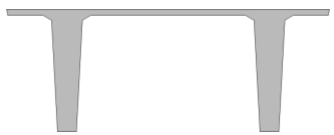							
	Steel	BFRP	Steel	BFRP	Steel	BFRP	Steel	BFRP
*g*1 [kN/m (klb/ft)]	12.26 (0.84)	11.97 (0.82)	9.27 (0.64)	9.06 (0.62)	5.18 (0.36)	5.07 (0.35)	8.52 (0.58)	8.39 (0.58)
Type of non-struct. load	skylights		skylights		tech. fin. pack.		tech. fin. pack.	
g2 [kN/m (klb/ft)]	0.50 (0.03)		0.50 (0.03)		2.90 (0.20)		6.25 (0.43)	
Type of imposed load	snow		snow		crowd		crowd	
q [kN/m (klb/ft)]	6.00 (0.41)		6.00 (0.41)		4.63 (0.32)		10.00 (0.69)	
SLS load [kN/m (klb/ft)]	18.76 (1.29)	18.47 (1.27)	15.77 (1.08)	15.56 (1.07)	12.71 (0.87)	12.60 (0.86)	24.77 (1.70)	24.64 (1.69)
USL load [kN/m (klb/ft)]	25.58 (1.75)	25.21 (1.73)	21.70 (1.49)	21.42 (1.47)	17.45 (1.20)	17.31 (1.19)	34.20 (2.34)	34.03 (2.33)

Constitutive modeling of materials

Concrete class C70/85 with PP fibers

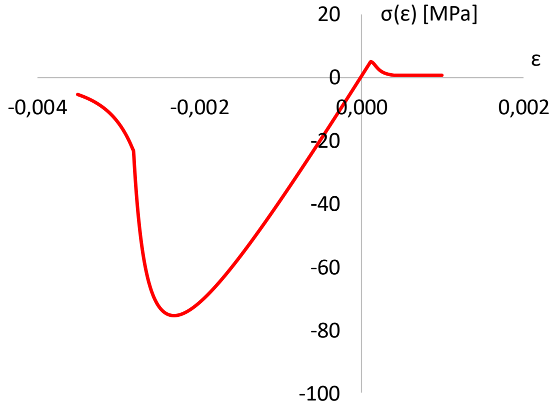

f_{ck} = 70 MPa
ε_{c1} = 0.0020
ε_{cu} = 0.0035
σ_{ctf} = 0.51 Mpa
ε_{cel} = 0.0015

γ_m = 1.40
(NTC 2018)

E = 45 GPa
f_{ptk} = 1098 MPa
ε_{puk} = 2,46%

γ_m = 1.25
(FIB 2010)

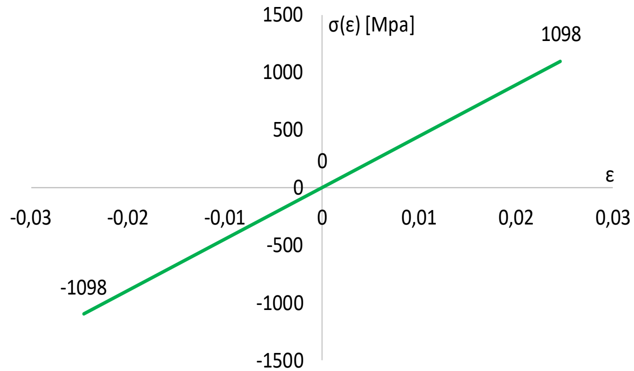

BFRP in bars

Prestressing steel in tendons

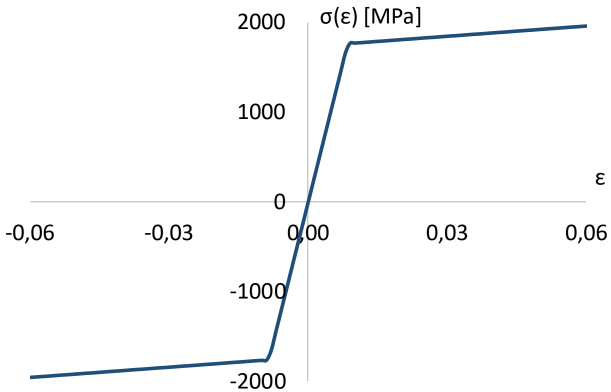

E_{pk} = 200 GPa
$f_{p0.1k}$ = 1770 MPa
f_{ptk} = 1960 MPa
ε_{puk} = 0.060

γ_m = 1.15
(NTC 2018)

Design criteria

Stress at demold (1/2 day with heat cycle)

$$\sigma_t < f_{ctj}$$

$$\sigma_c < 0{,}7 \cdot f_{ckj}$$

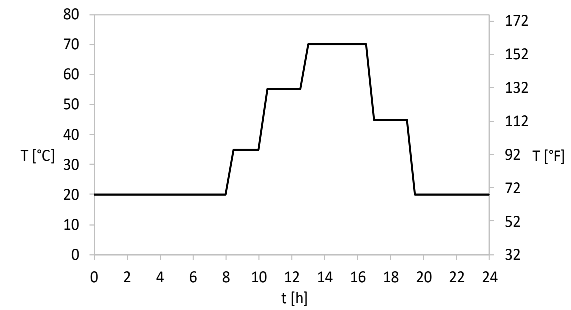

ULS bending strength

$$N = \int_0^h \sigma_c(\varepsilon) \cdot b(y) \cdot dy + \sum_{k=1}^{jp} \sigma_p(\varepsilon + \bar{\varepsilon}_i) \cdot Ap_k$$

$$M = \int_0^h \sigma_c(\varepsilon) \cdot b(y) \cdot (y - y_G) \cdot dy + \sum_{k=1}^{jp} \sigma_p(\varepsilon + \bar{\varepsilon}_i) \cdot (\bar{y}_k - y_G) \cdot Ap_k$$

SLS deflection (demoulding, storage, assemblage, end of service life)

$$v(x,t) = v_M + v_{g1} + v_{g2} + v_q + \int_0^t \frac{d\Phi(\bar{t}, t_0)}{d\bar{t}} \cdot (v_M + v_{g1}) \cdot d\bar{t} + \int_{t_2}^t \frac{d\Phi(\bar{t}, t_0 + t_2)}{d\bar{t}} \cdot v_{g2} \cdot d\bar{t}$$

- $L/500 < v1(t_0) < 0$ - $L/500 < v1(t_2) < 0$

- $L/500 < v2(t_2) < 0$ - $L/500 < v2(t_u) < 0$

- $L/500 < v_{max}(t_u) <$ - $L/300$

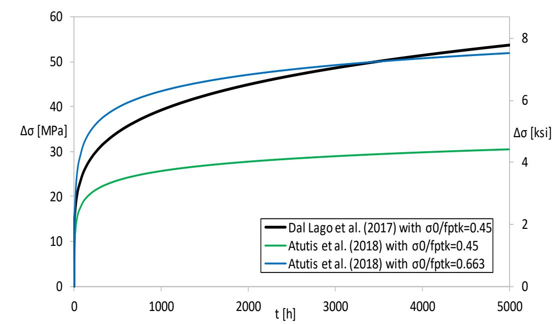

Comparison of geometry and reinforcement

								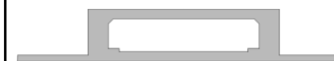	
	Steel	BFRP	BFRP*	Steel	BFRP	Steel	BFRP	Steel	BFRP
b_{max} [m (ft)]	2.498 (8.196)	2.498 (8.196)	2.498 (8.196)	2.500 (8.202)	2.500 (8.202)	1.200 (3.937)	1.200 (3.937)	2.500 (8.202)	2.500 (8.202)
A_c [m² (ft²)]	0.486 (5.231)	0.486 (5.231)	0.481 (5.178)	0.365 (3.929)	0.363 (3.907)	0.205 (2.207)	0.205 (2.207)	0.341 (3.671)	0.341 (3.671)
A_p [m² (ft²)]	0.01235 (0.133)	0.01295 (0.139)	0.01800 (0.194)	0.01261 (0.136)	0.01390 (0.150)	0.00677 (0.073)	0.00604 (0.065)	0.00807 (0.087)	0.00865 (0.093)
$N_{tendons}$ [-]	16ϕ0.6″ 8ϕ0.5″	16ϕ16 8ϕ12	24ϕ16 8ϕ12	22ϕ0.6″	22ϕ16	17ϕ0.5″	17ϕ12	12ϕ0.6″ 3ϕ0.5″	12ϕ16 3ϕ12

* Prestressed with more BFRP bars

Comparison of sectional behavior

								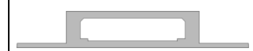	
	Steel	BFRP	BFRP*	Steel	BFRP	Steel	BFRP	Steel	BFRP
M_{Rd} [kNm (klb·ft)]	4927 (3623) 4856† (3571)†	3003 (2208) 2925† (2151)†	4077 (2998) 3830† (2816)†	4557 (3351) 4504† (3312)†	2904 (2135) 2866† (2107)†	931 (685) 915† (673)†	588 (432) 570† (419)†	1301 (957) 1269† (933)†	941 (692) 911† (670)†
$\chi_{ultimate}$ [10^{-3}/m (10^{-3}/in)]	50.84 (1.29) 52.00† (1.32)†	13.06 (0.33) 13.07† (0.33)†	13.60 (0.35) 12.24† (0.31)†	8.02 (0.20) 8.25† (0.21)†	11.93 (0.30) 12.27† (0.31)†	50.16 (1.27) 51.30† (1.30)†	34.56 (0.88) 34.38† (0.87)†	45.92 (1.17) 47.39† (1.20)†	35.89 (0.91) 35.85† (0.91)†
$\varepsilon_{c,max}$ [%]	**0.319**	0.097	0.125	**0.290**	**0.350**	**0.318**	0.101	**0.347**	0.198
$\varepsilon_{R,max}$ [%]	5.2	**2.5**	**2.5**	1.1	2.2	2.2	**2.5**	2.0	**2.4**

* Prestressed with more BFRP bars

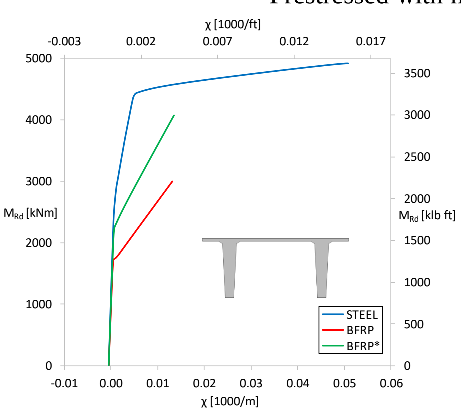

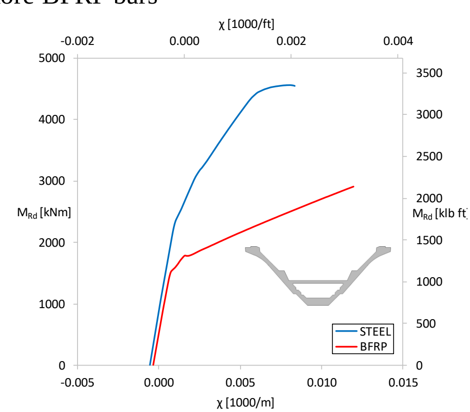

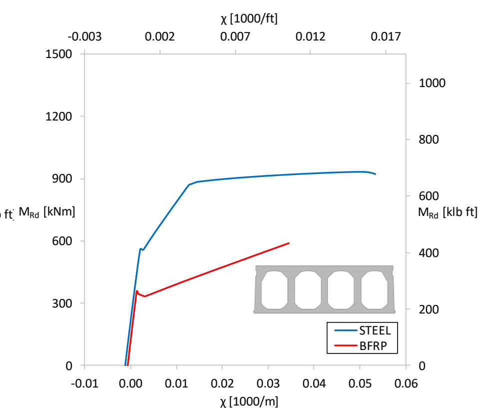

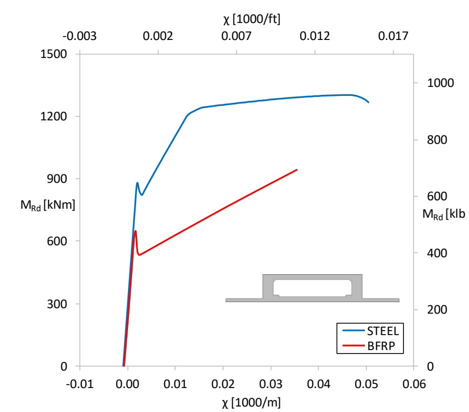

Comparison of loss evolution

STEEL

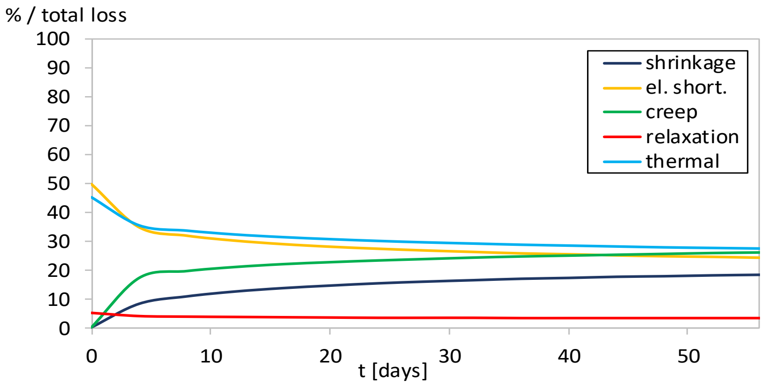

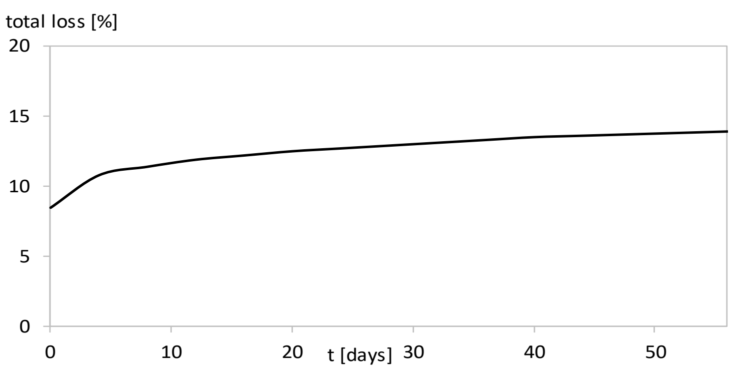

Low loss for relaxation (ρ_{1000} = 2,5%)

High loss for shortening (E = 200 GPa)

BFRP

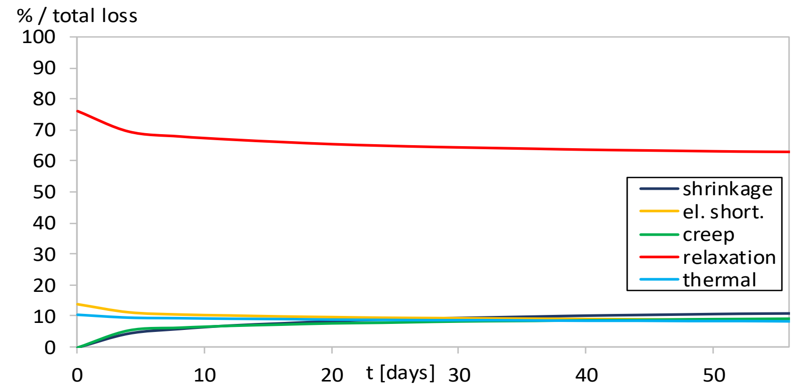

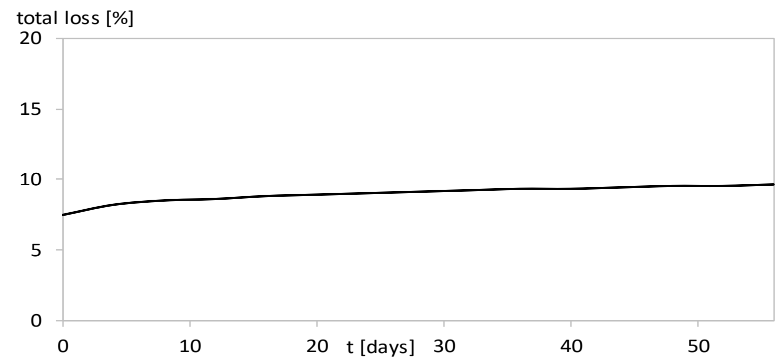

High loss for relaxation (ρ_{1000} = 8,4%)

Low loss for shortening (E = 48 GPa)

Mean 50-year loss for both at 16~19%

e.g. TT element

Comparison of maximum span

						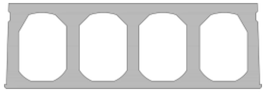			
	Steel	BFRP	BFRP*	Steel	BFRP	Steel	BFRP	Steel	BFRP
L_{max} [m (ft)]	32.0 (105.0)	27.0 (88.6)	32.0 (105.0)	31.0 (101.7)	25.5 (83.7)	18.0 (59.1)	13.5 (44.3)	15.5 (50.9)	12.5 (41.0)
$\frac{L_{max,BFRP}}{L_{max,STEEL}}$	0.84 (1.00*)			0.82		0.75		0.81	

* Prestressed with more BFRP bars

Conclusions

The maximum attainable span of all cross-sections has always been determined by SLS checks, rather than by ULS;

The checks of the elastic stresses at prestressing release are determinant for the cross-sectional maximum reinforcement;

- elastic compressive stresses at prestressing release are critical especially for the TT, wing-shaped and hollow core sections;
- Elastic tensile stresses at prestressing release are critical especially for wing-shaped sections;

The camber limitations have been critical mainly for the elements prestressed with BFRP due to the shorter span needed for a deflection control over time;

The level of prestressing losses is very similar among the different sections and reinforcement types, despite for steel tendons the progressive beam shortening constitutes the predominant loss mechanism, whilst for BFRP bars relaxation constitutes the predominant loss mechanism

Conclusions

Given BFRP bars act elastically up to a state of incipient collapse, they never lose the prestressing effect, whilst the steel tendons lose it after the conventional yielding strain;

The replacement of steel tendons with BFRP bars generally brings to a relevant reduction of both ultimate strength and curvature due to the lower tensile strength and to the brittle mechanical behavior of the BFRP bars: max span reduction 25% - compatible with several uses mainly when durability is of concern.

Prestressed BFRP bars are suitable for applications in precast industry:

- the TT section is the only one where a higher number of BFRP bars could be placed with positive effects, bringing to a limit situation with the same span as the element reinforced with steel, and thus it can be selected as the most performing for the use of prestressed BFRP bars.
- The hollow core section provided the maximum span reduction and is therefore the less performant for the replacement of steel tendons with BFRP bars.
- the wing-shaped section appears to be the most balanced one with respect to the bending resistance, with concrete failure occurring with BFRP at incipient failure;

THANK YOU FOR YOUR ATTENTION!